

High-power traveling wave photodetector in silicon photonics with monolithically integrated optical power splitter

L. Bogaert,^{1,2} K. Van Gasse,² G. Torfs,¹ J. Bauwelinck¹ and G. Roelkens²

¹ IDLab, INTEC, Ghent University - imec, 9052 Ghent, Belgium

² Photonics Research Group, INTEC, Ghent University - imec, 9052 Ghent, Belgium

Photodetectors suffer from a limited maximum RF output power. To boost the maximum photodetector RF output power while maintaining a high bandwidth, we designed traveling wave photodetectors (TWPDs) integrated on a silicon photonics platform. By carefully matching the delay in the optical and electrical domain, constructive addition maximizes the output power. Additionally, a monolithically integrated star coupler is added to the design to limit the optical power in the waveguides and hereby preserve the high linearity introduced by the TWPD. In this paper, focus will be on the TWPD itself, for which bandwidth and impedance measurements will be presented.

Introduction

The ever-increasing demand for high-speed wireless data connectivity requires new wireless network infrastructure. Decreasing cell sizes and migrating towards (near-) millimeter wave frequencies [1] will play a major role in obtaining those higher data rates. To make these solutions economically viable, a centralized approach will be required. In literature, Radio-over-Fiber [2] has been proposed to transfer the radio signal generated at the central office (CO) to the desired remote antenna unit (RAU). Subsequently, a conversion from the optical domain to the electrical domain will take place in the RAU, which is typically done by a photodetector (PD) followed by a transimpedance amplifier. Alternatively, the electrical amplification can be shifted to the optical domain where it can be done in the CO for multiple RAUs at once, significantly reducing the RAU complexity and power consumption. Unfortunately, PDs suffer from a limited maximum RF output power [3]. Combining multiple PDs in parallel relaxes the saturation limit of the opto-electrical conversion at the cost of a significant drop in bandwidth. To boost the maximum photodetector RF output power while maintaining a high bandwidth, we designed traveling wave photodetectors (TWPDs) [4] integrated on a silicon photonics platform.

Proposed architecture

The monolithically integrated TWPD that is discussed in this paper is depicted schematically in Fig. 1. From input to output it consists of an optical splitter, optical delay elements and dual fed PDs embedded in a transmission line. The optical splitter used in this design is a monolithically integrated star coupler [5] rather than an optical power splitting tree consisting of 50-50 power splitters. This is done to limit the optical power coupled to a single waveguide and hereby preserve the high linearity introduced by the TWPD. Additionally, the star coupler provides a more compact solution, effectively reducing the cost of the receiver.

In the design shown in Fig. 1, the transmission line is terminated by a dummy load. This dummy load should ideally be equal to the impedance of the loaded transmission line and will absorb the backward propagating waves in the TWPD. Without the presence of such a dummy load, backward propagating waves will reflect at the position of the dummy load. Consequently, the backward propagating waves will couple with the

forward propagating waves in the absence of such a dummy load. Those interference effects will be cancelled by the dummy load resulting in a higher bandwidth at the cost of an inherent 6 dB loss.

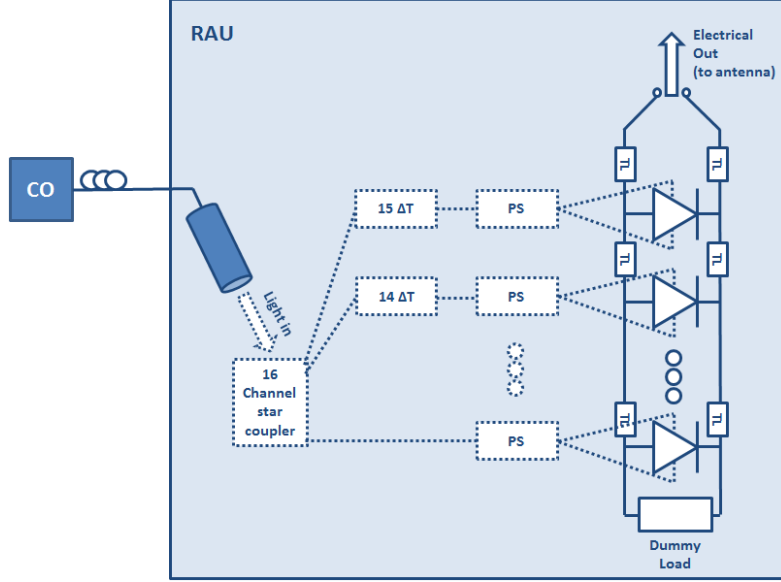


Figure 1: Proposed architecture (PS: Power Splitter, TL: Transmission line)

The first major criterion to take into account while designing the TWPD, is that the unloaded transmission line should be designed in such a way that after loading the transmission line periodically with PDs, the transmission line should have a characteristic impedance (eq. (1))[4] equal to the targeted load impedance. L_{TL} and C_{TL} are parameters of the unloaded transmission line and respectively denote the “per unit length inductance” and “per unit length capacitance”. The other two parameters in eq. (1) depend on the loading of the TWPD, where C_j describes the junction capacitance of the PD and Δl_{el} is the spacing between consecutive PDs.

$$Z_{0,Loaded\ TL} = \sqrt{\frac{L_{TL}}{C_{TL} + (C_j/\Delta l_{el})}} \quad (1)$$

Secondly, to get an optimal power transfer from the TWPD to the load, the delay in the optical and electrical domain should be matched carefully (eq. (2)) such that the RF signal generated in the different PDs combines constructively at the output. The velocity of the RF signal on the loaded transmission line (v_{el}) is given by eq. (3)[4]. On the other hand, Δl_{opt} (the difference in optical delay between consecutive PDs) and $v_{opt,g}$ (group velocity of the optical signal) will be determined by the optical power distribution part of the circuit.

$$\frac{\Delta l_{el}}{v_{el}} = \frac{\Delta l_{opt}}{v_{opt,g}} \quad (2) \quad \frac{1}{v_{el}} = \sqrt{L_{TL} \cdot \left(C_{TL} + \frac{C_j}{\Delta l_{el}} \right)} \quad (3)$$

The TWPD discussed in the remainder of this article was designed for a 50 Ω load. However, an error in the design phase resulted in the fact that the PD spacing was

chosen too small. Consequently, the per unit length contribution of the junction capacitance of the PD was too high resulting in a characteristic impedance of 35.4Ω for the loaded transmission line.

Frequency dependence

The frequency dependence of the receiver structure was measured as part of a back-to-back transceiver link (Fig. 2). Consequently, the bandwidth is not only determined by the receiver structure, but also by the Mach-Zehnder modulator (MZM) used for modulating the signal at the transmitter side. To calibrate out the transmitter side, a reference measurement was done with a high bandwidth on-chip PD (with a specified bandwidth of at least 45 GHz) for which it was assumed that all the frequency dependent effects are caused by the MZM. The measured S_{21} curve of this high bandwidth PD was then subtracted from the measured S_{21} curves of the other structures to obtain the S_{21} plots depicted in Fig. 3. It is important to remark that the high bandwidth PD was only used for calibration purposes. The four structures given in Fig. 3, are using a different PD which has a higher responsivity at the cost of a lower bandwidth.

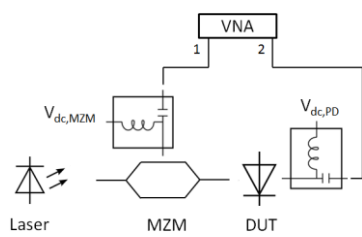


Figure 2: Setup for S_{21} measurements

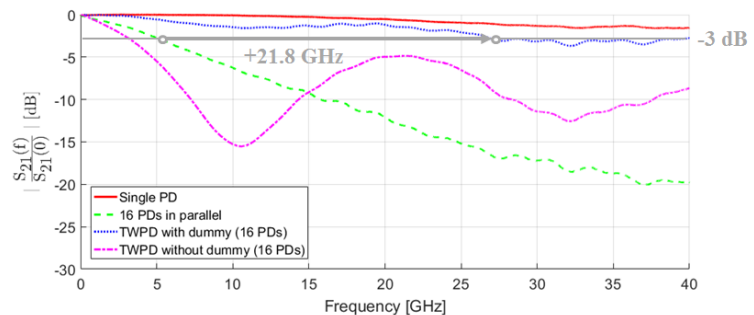


Figure 3: Measured S_{21} after normalization (2V reverse voltage)

It can be seen (Fig. 3) that adding multiple PDs in shunt drastically decreases the bandwidth. Using a TWPD is a way to combine multiple PDs without sacrificing too much bandwidth. When comparing the TWPD with and without dummy load, one can clearly see (Fig. 3) that adding a dummy load resolves the interference effects, resulting in a higher bandwidth. For a fair comparison, simulation results are shown (Fig. 4) where the amount of incident light is kept constant. One can clearly see the increase in bandwidth at the cost of an inherent 6 dB loss when adding a dummy load. The latter is caused by the fact that the dummy load absorbs half of the current generated in the PDs.

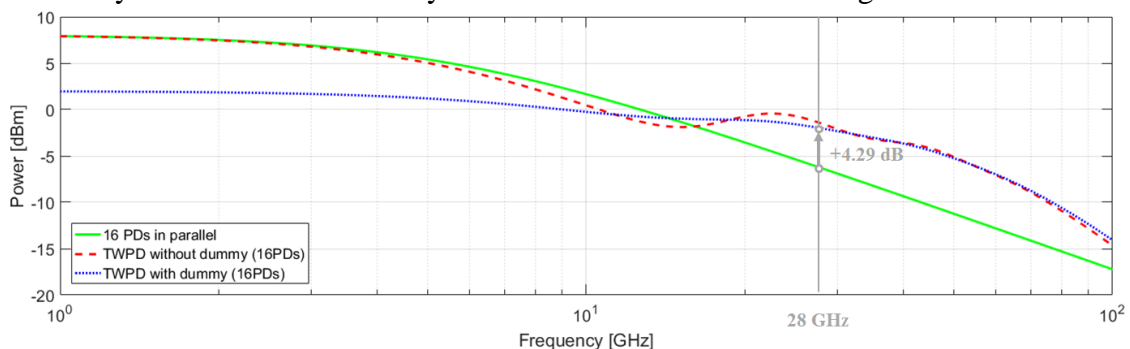


Figure 4: Simulated output power of the different structures when each PD generates 1 mA peak current (2V reverse voltage)

Output impedance of the traveling wave photodetectors

In this section the output impedance of two types of TWPDs are given, namely the TWPD with and without dummy load (Fig. 5). As mentioned previously, the realized characteristic impedance is 35.4Ω and thus the S-parameters depicted below are given for a reference impedance of 35.4Ω . Adding a dummy load to the TWPD results in an output impedance which is nicely matched over the whole measured frequency range. On the other hand, it is clear that the S-parameters for the variant without dummy load describe the expected behavior for a lossy transmission line with an open termination. While the dummy load is specified to be 50Ω , it is clear from the S-parameters given in Fig. 5 that the DC impedance of the TWPD deviates from the expected 50Ω . This can be attributed to the on-chip 50Ω dummy, whose resistance value changes strongly in function of the DC voltage applied over the TWPD (64.5Ω at 2V reverse voltage).

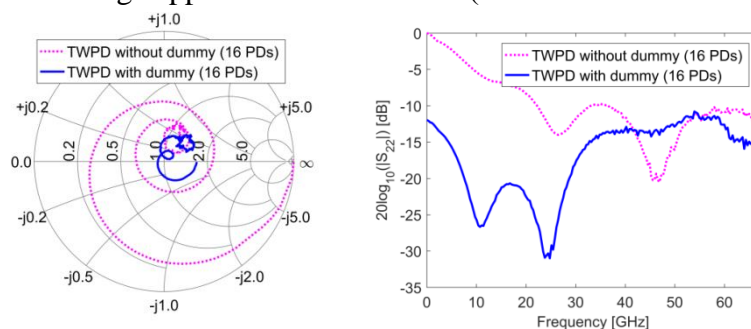


Figure 5: Measured S_{22} (reflectivity at the electrical output) at 2V reverse voltage ($Z_{\text{ref}} = 35.4 \Omega$)

Conclusion

Centralization is key in making future wireless network architectures scalable. Amplification is nowadays performed at the antenna after the conversion from the optical to electrical domain. A shift towards centralization via the use of optical amplification at the central office is hindered by the limited power capabilities of a PD. Dividing the optical power at the antenna between multiple parallel PDs increases the maximum obtainable power level at the cost of a major drop in bandwidth. For Radio-over-Fiber it is therefore advisable to adopt a TWPD structure which combines multiple PDs in such a way that it preserves high speed operation.

Acknowledgements

This work was supported by the Ghent University Special Research Fund, project BOF14/GOA/034.

References

- [1] J. G. Andrews et Al., "What Will 5G Be?," *IEEE J. Sel. Areas Commun.*, Vol. 32, 1065-1082, 2014.
- [2] V.A. Thomas, M. El-Hajjar, and L. Hanzo, "Performance Improvement and Cost Reduction Techniques For Radio Over Fiber Communications," *IEEE Commun. Surveys Tuts.*, Vol. 17, 627-670, 2015.
- [3] P. Liu, K. J. Williams, M. Y. Frankel, and R. D. Esman, "Saturation Characteristics of Fast Photodetectors," *IEEE Trans. Microw. Theory Techn.*, Vol. 47, 1297-1303, 1999
- [4] L. Y. Lin et Al., "High-Power High-Speed Photodetectors – Design, Analysis, and Experimental Demonstration," *IEEE Trans. Microw. Theory Techn.*, Vol. 45, 1320-1331, 1997
- [5] T. Spuesens, S. Pathak, M. Vanslembrouck, P. Dumon, and W. Bogaerts, "Grating Couplers With an Integrated Power Splitter for High-Intensity Optical Power Distribution," *IEEE Photon. Technol. Lett.*, Vol. 28, 1173-1176, 2016.